Journal of Southeast University (English Edition) Vol. 33, No. 1, pp. 101 - 105 Mar. 2017 ISSN 1003—7985

Design and laboratory evaluation of fog-sealed chip seal on epoxy asphalt pavement for steel bridge deck

Zheng Dong[1] Qian Zhendong[1] Wang Rui[2] Liu Yang[1]

([1]Intelligent Transportation System Research Center, Southeast University, Nanjing 210096, China)

([2]Administrant Department of Suzhou Highway, Suzhou 215007, China)

Abstract: In order to improve the surface performance of epoxy asphalt pavement (EAP) for steel bridge deck, an epoxy asphalt chip seal (ECS) covered by a cationic emulsified asphalt fog seal (i. e., fog-sealed chip seal) is proposed and a laboratory study is conducted to design and evaluate the fog-sealed chip seal. First, the evaluation indices and methods of the chip seal on steel bridge deck pavement were proposed. Secondly, the worst pavement conditions during the maintenance time were simulated by the small traffic load simulation system MMLS3 and the short-term aging test for minimizing the failure probability of chip seal. Finally, the design parameters of fog-sealed chip seal were determined by the experimental analysis and the performance of the designed fog-sealed chip seal was evaluated in the laboratory. Results indicate that the proposed simulation method of pavement conditions is effective and the maximal load repetitions on the EAP slab specimen are approximately 925 300 times. Moreover, the designed fog-sealed chip seal can provide a dense surface with sufficient skid resistance, aggregate-asphalt adhesive performance and interlayer shearing resistance.

Key words: pavement maintenance; composite seal; epoxy asphalt; laboratory evaluation; pavement condition simulation; steel bridge deck pavement

DOI: 10.3969/j.issn.1003-7985.2017.01.017

Epoxy asphalt pavement (EAP) has been widely applied to the steel bridges in China due to its good physical and mechanical properties[1]. However, surface distresses still occur in the EAP layer of some steel bridges and eventually lead to pavement structure failure if lacking effective maintenance[2-3]. Besides, the EAP, generally composed of suspended-dense structure, tends to cause insufficient skid resistance on rainy days[4]. Therefore, a suitable maintenance treatment is necessary for the in-service EAP.

In recent years, much research has focused on chip seals for asphalt pavement maintenance. To eliminate the major problems appearing in the application of chip seal, such as loose aggregate and poor interlayer shearing resistance, two primary approaches have been studied, including the application of the composite seal and polymer modified asphalt[5-7]. Im and Kim[8] applied the fog seal onto the chip seal to solve the problem of loose aggregates. Duan[9] analyzed the SBS modified bitumen synchronous chip seal to solve the problem of the sticking wheel. However, few efforts have been made to combine the two approaches and simulate the conditions of asphalt pavement when evaluating the performance of the seal coat in the laboratory.

Epoxy asphalt is a thermosetting material, composed of epoxy resin (component A), curing agent and asphalt (component B). Mixed with the aggregates, epoxy asphalt provides excellent stability and stiffness for the mixture[10]. Although the cost of epoxy asphalt is high, if a 10-years or more service life is achieved, the epoxy asphalt chip seal (ECS) can provide cost-effective alternatives from the aspect of life-cycle cost[11]. In addition, fog seal is superior to the slurry seal due to its low cost and fast construction[12]. If the fog seal is applied in the composite seal instead of slurry seal, the composite seal will have better economic effectiveness and workability.

The objective of this study is to design an ECS layer covered by a cationic emulsified asphalt (CEA) fog seal (i. e., fog-sealed chip seal) and to evaluate the properties of the fog-sealed chip seal in the laboratory, including the skid resistance, imperviousness, aggregate-asphalt adhesive performance and interlayer shearing resistance.

1 Materials and Design Method

1.1 ECS

In this study, ECS was composed of epoxy asphalt binder and basalt aggregate. The epoxy asphalt binder was obtained from a US manufacturer and the basalt aggregate was produced in Jiangsu Province, China. The technical indices of basalt aggregate and epoxy asphalt binder are listed in Tab. 1.

Received 2016-08-20.

Biographies: Zheng dong (1990—), male, graduate; Qian Zhendong (corresponding author), female, doctor, professor, qianzd@seu.edu.cn.

Foundation item: The National Natural Science Foundation of China (No. 51378122).

Citation: Zheng Dong, Qian Zhendong, Wang Rui, et al. Design and laboratory evaluation of fog-sealed chip seal on epoxy asphalt pavement for steel bridge deck[J]. Journal of Southeast University (English Edition), 2017, 33(1): 101 - 105. DOI: 10.3969/j.issn.1003-7985.2017.01.017.

Tab. 1 Technique indices of the raw materials

Materials	Technical indices	Value
Basalt aggregate	Density/(g · cm^{-3})	2.97
	Polished stone value	52
	Acicular content/%	1.0
	Crushing value/%	8.9
Epoxy asphalt binder	Mass ratio of components A and B	100∶296
	Tensile strength/MPa	9.7
	Fracture elongation/%	190
	Viscosity from 0 to 1 Pa · s/min	25

Two gap gradations of ECS are designed in this study, including the single sized gravel gradation (S-ECS) and the graded gravel gradation (G-ECS). The gradation curves of different mixtures are shown in Fig. 1.

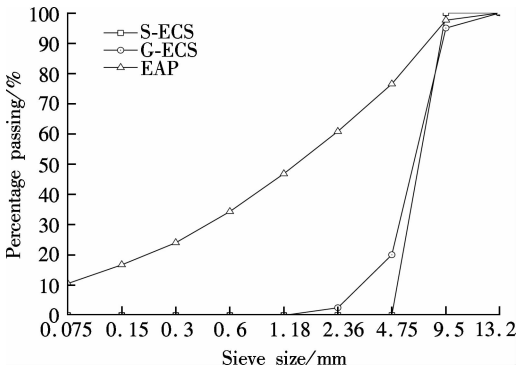

Fig. 1 Gradation curves of different mixtures

The Mcleod method is adopted in this study to determine the design parameters of ECS.

$$\left.\begin{aligned} C &= (1-0.4V)\times \mathrm{ALD}\times G\times E \\ V &= 1-\frac{W}{G} \\ H &= \frac{M}{1.139\,285+0.011\,506\mathrm{FI}} \\ B &= (0.4HTV+S+A)\rho \end{aligned}\right\} \quad (1)$$

where C is the aggregate application rate; B is the asphalt application rate; W is the accumulated density of the aggregates; G is the density of aggregates; V is the percent voids in aggregates; M is the median particle size of the gap-graded aggregates; FI is the acicular content of the aggregates; ALD is the average least design dimension of the aggregates; E is the loss coefficient of the aggregates; T is the correction factor of the traffic volume; S is the correction factor of road condition; A is the absorption of aggregates; ρ is the density of the asphalt binder.

The design results of S-ECS and G-ECS are listed in Tab. 2 and Tab. 3, respectively.

Tab. 2 Aggregate application rates of S-ECS and G-ECS

Material	G/(kg · m^{-3})	W/(kg · m^{-3})	V/%	M/mm	FI/%	ALD/mm	E	C/(kg · m^{-2})
S-ECS	2 970	1 610	45.8	7.1	1.0	6.2	1.1	16.5
G-ECS	2 970	1 630	45.1	5.5	1.0	4.8	1.1	12.9

Tab. 3 Asphalt application rates of S-ECS and G-ECS

Material	ALD/mm	V/%	T	S	A/%	ρ/(kg · m^{-3})	B/(kg · m^{-2})
S-ECS	6.2	45.8	0.6	0.14	0.71	1.01	0.84
G-ECS	4.8	45.1	0.6	0.14	0.65	1.01	0.67

1.2 CEA fog seal

In the research, the fog seal is made of CEA mixed by SK-90 bitumen, Emulsifier 18331 and purified water. The technical indices of CEA are listed in Tab. 4.

Tab. 4 Technique indices of CEA

Technical indices	Value	Technical requirements
Negra viscosity/MPa	8	1 to 10
Storage stability/%	0.2	≤1
Evaporation residue content/%	51	≥50
Evaporation residue ductility/cm	140	≥40
Evaporation residue needle/0.1 mm	83.3	40 to 120

Additionally, the CEA fog seal was designed by the British pendulum number test and wet track abrasion test. First, the British pendulum number test was used to select the initial design parameters (i.e., coating times and asphalt application rates). Subsequently, the wet track abrasion test was carried out to determine the ultimate design parameters of the CEA fog seal, following the procedure in JTG E20—2011[13]. Due to the light weight of the CEA fog seal, the abrasion ratio r_a was adopted instead of the wet track abrasion loss and measured by the plastic plate. The diagrammatic sketch of the plastic plate is shown in Fig. 2 and r_a can be calculated as

$$r_a = \frac{N_a}{N} \quad (2)$$

where N_a is the number of circular holes where exposed aggregates can be observed; N is the total number of circular holes, $N = 25$.

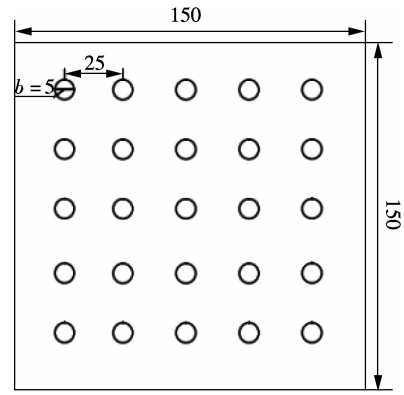

Fig. 2 Plastic plate for the test (unit: mm)

2 Experimental Design

2.1 Preparation of the EAP slab specimens

To evaluate the performance of the fog-seal chip seals

accurately, the pavement conditions of EAP during the maintenance time were simulated, including the traffic loads and asphalt aging.

First, the EAP slab specimen was prepared using the epoxy asphalt mixture processed by the short-term aging test in accordance with JTG E20—2011[13]. Subsequently, a third-scale model mobile loading simulator MMLS3 with the contact pressure of 0.7 MPa was used to load on test specimens (300 mm × 150 mm × 50 mm) sawn from the EAP slab specimen at 35 ℃. After loading a certain number of times, the standard British pendulum number F_{B20} was measured using a British Pendulum Tester. Then, the skid resistance decay curve was fitted by the Asymptotic model[14], and the minimum acceptable baseline was determined according to the threshold value of F_{B20} for the steel bridge deck pavement (≥45). Finally, the maximal load repetitions was calculated by the benefit-cost ratio method, and the EAP slab specimen can be prepared for the design of fog-sealed chip seals by simulating the asphalt aging and maximal load repetitions. The Asymptotic model is

$$y = Ae^{Bx} + C \qquad A, C > 0; B < 0 \tag{3}$$

and the procedure of the MMLS3 test can be summarized in Fig. 3.

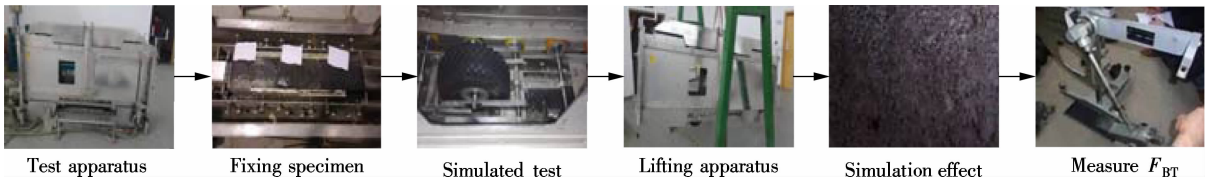

Fig. 3 Procedure of the MMLS3 test

2.2 Evaluation indices and test method

The fog-sealed chip seal should have sufficient structure strength, which is affected by the aggregate-asphalt adhesive performance. In addition, superior imperviousness of the fog-sealed chip seal can protect the EAP and excellent skid resistance is beneficial for ensuring driving safety. Similarly, the interlayer shearing resistance has a vital effect on the synergy between the composite seal and asphalt pavement[15]. Therefore, the gravel loss rate L_g, shear strength S_s, water permeability coefficient C_w, F_{B20} and mean texture depth (MTD) are chosen as evaluation indices to analyze the aggregate-asphalt adhesive performance, imperviousness, interlayer shearing resistance and skid resistance of the fog-sealed chip seal, respectively.

In this study, L_g was measured by the low-temperature adhesion test according to JTG E20—2011[13], using the fully-cured chip seal sample. L_g can be calculated by

$$L_g = (W_f - W_i)/W_i \times 100\% \tag{4}$$

where W_f and W_i are the sample weight before and after the test, respectively.

Moreover, S_s was measured by the skew shearing test. The test specimen was manufactured by two cuboid specimens (5 cm × 5 cm × 2.5 cm) sawn from the EAP slab specimen, bonded with epoxy asphalt binders. Furthermore, the fully-cured test specimen was put into the thermostatic water tank of 60 ℃ for 30 min, and then the skew shear test was conducted at 60 ℃ with the loading rate of 500 mm/min and the shear angle of 45°.

Additionally, C_w was measured by the seepage test, following the procedure in JTG E20—2011[13]. F_{B20} was measured with a British Pendulum Tester, and MTD was measured by the sand-patch test, following the procedure in JTG E20—2011[13].

3 Test Results and Discussion

3.1 Simulation of pavement conditions

The results of F_{B20} measured by the MMLS3 test are shown in Fig. 4. It can be found that the maximal load repetitions are approximately 925 300 times.

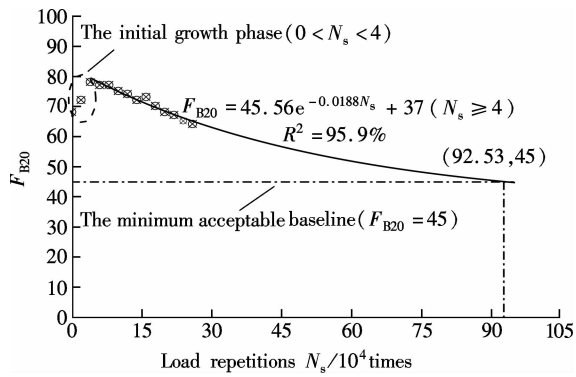

Fig. 4 Results of F_{B20} with load repetitions

To verify the effectiveness of the proposed simulation method, the skid resistance of the simulated EAP and the relationship between the theoretical and trial F_{B20} values are illustrated in Fig. 5 and Fig. 6, respectively. It can be found that the theoretical F_{B20} values are fairly close to the trial F_{B20} values and the R^2 value is greater than 99%. Additionally, some polished aggregates and aged asphalt binders can be observed from the specimen surface after the test, basically corresponding with the actual surface status of the in-service EAP. These results indicate that the proposed method is capable of simulating the pavement conditions.

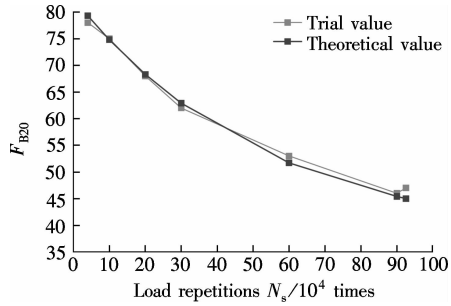

Fig. 5 Comparison of theoretical and trial F_{B20} values

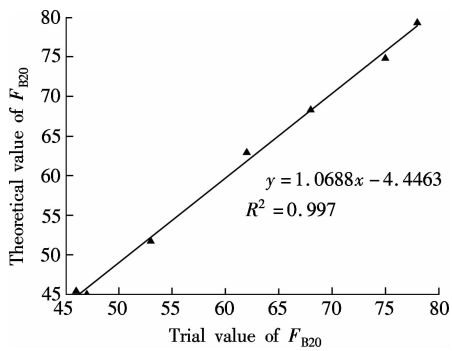

Fig. 6 Relationship between of the theoretical and trial F_{B20} values

3.2 Analysis of design parameters

3.2.1 ECS

The properties of S-ECS and G-ECS measured in the laboratory are listed in Tab. 5. The skid resistance (both MTD and F_{B20}) is improved significantly after ECS construction. In addition, the L_g value of each ECS is less than 20% and the shear strength of each ECS is greater than 0.7 MPa (threshold value in the steel bridge deck pavement), indicating sufficient aggregate-asphalt adhesive performance and shear strength of ECS. On the contrary, the C_w value of each ECS is about 2 to 6 times that of EAP, revealing the poor imperviousness of ECS, particularly S-ECS. Based on the above analysis, G-ECS is chosen as the structure of the chip seal in this study.

Tab. 5 Properties of S-ECS and G-ECS

Evaluation indices	EAP	S-ECS	G-ECS
MTD/mm	0.31	0.93	0.80
F_{B20}	47	85	81
C_w/(mL · min^{-1})	5.0	33.9	13.3
L_g/%		13.6	15.3
S_s/MPa		0.87	0.83

3.2.2 CEA fog seal

The skid resistance of the CEA fog seal with various application rates and coating times is shown in Fig. 7. It can be observed that the CEA application rates of 0.35 and 0.4 L/m^2 and the coating times of one and two can provide better skid resistance for the CEA fog seal compared with other design parameters. Subsequently, the CEA fog seal (CEA application rate is 0.4 L/m^2; two coating times) is chosen using the wet track abrasion test

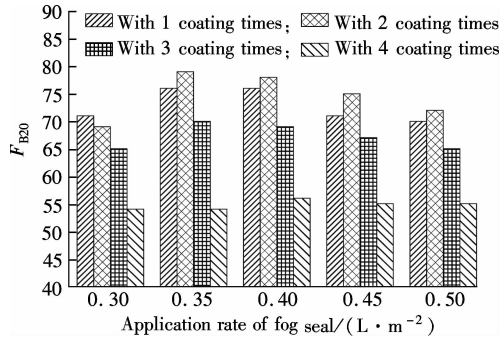

Fig. 7 Test results of the skid resistance of CEA fog seal

due to the minimum value of r_a (3/25).

To sum up, the ultimate maintenance strategy in this study was the fog-sealed chip seal composed of the G-ECS ($C = 12.9$ kg/m^3; $B = 0.67$ kg/m^3) and the CEA fog seal (CEA application rate is 0.4 L/m^2; two coating times).

3.3 Performance evaluation

The properties of the designed fog-sealed chip seal were measured by five evaluation tests, and r_c was defined as the change ratio to analyze the discrepancies of each evaluation index. r_c can be calculated by

$$r_c = \frac{\Delta I}{I_0} \times 100\% \quad (5)$$

where I is the variation of the evaluation index; I_0 is the initial value of the evaluation index. The results of five evaluation tests are shown in Tab. 6.

Tab. 6 Properties of the designed fog-sealed chip seal

Evaluation indices	Initial value of G-ECS	Fog-sealed chip seal	
		Value	r_c/%
MTD/mm	0.80	0.76	−5.0
F_{B20}	81	78	−3.7
C_w/(mL · min^{-1})	13.3	3.3	75.2
L_g/%	15.3	0.7	95.4
S_s/MPa	0.83	0.84	1.2

From Tab. 8, the C_w value of the designed fog-sealed chip seal is less than that of G-ECS and the r_c value is 75.2%, suggesting that the imperviousness of the fog-sealed chip seal is excellent compared with G-ECS. The reason is that asphalt binders of the CEA fog seal fill in the voids between the aggregates and form a closed layer on G-ECS to prevent water from entering the underlying layer. In addition, the gravel loss rate is close to 0 and the r_c value is 95.4% after CEA fog seal construction, which indicates that the fog-sealed chip seal can eliminate the problem of loose aggregates effectively. In contrast, after coating the CEA fog seal on G-ECS, the skid resistance declines slightly and the interlayer shearing resistance remains almost unchanged. Therefore, the designed fog-sealed chip seal has sufficient skid resistance, imperviousness and a relatively long service life provided by an excellent aggregate-asphalt adhesive performance and interlayer shearing resistance.

4 Conclusion

The proposed simulation method of in-service EAP is effective and the maximal load repetitions on the EAP slab specimen are approximately 925 300 times. The designed fog-sealed chip seal consists of the G-ECS (C = 12.9 kg/m^3; B = 0.67 kg/m^3) and the CEA fog seal (asphalt application rate is 0.4 L/m^2; two coating times). According to the performance evaluation results, the designed fog-sealed chip seal can provide a dense surface with sufficient skid resistance and a relatively long service life.

References

[1] Huang W, Qian Z D, Cheng G. Application of epoxy asphalt concrete to pavement of long-span steel bridge deck [J]. *Journal of Southeast University (Natural Science Edition)*, 2002, **32**(5): 783-787. (in Chinese)

[2] Chen X H, Liu X Y, Qian Z D, et al. State-of-art of asphalt surfacings on long-spanned orthotropic steel deck in China [J]. *Journal of Testing and Evaluation*, 2012, **40**(7):663-681.

[3] Nega A, Nikraz H, Herath S, et al. Distress identification, cost analysis and pavement temperature prediction for the long-term pavement performance for Western Australia [J]. *International Journal of Engineering and Technology*, 2015, **7**(4): 267-275. DOI: 10.7763/ijet.2015.v7.803.

[4] Luo S, Qian Z D. Experimental research on surface characteristics of epoxy asphalt concrete pavement [J]. *Journal of Beijing University of Technology*, 2012, **38**(2): 219-222. (in Chinese)

[5] Aktaş B, Karaşahin M, Saltan M, et al. Effect of aggregate surface properties on chip seal retention performance [J]. *Construction and Building Materials*, 2013, **44**(3): 639-644. DOI: 10.1016/j.conbuildmat.2013.03.060.

[6] Hitti E. The R Factor: California project combines RAP and tire rubber in a cape seal treatment [J]. *Asphalt*, 2014, **29**(3):25-29.

[7] Gransberg D D, Zaman M. Analysis of emulsion and hot asphalt cement chip seal performance [J]. *Journal of Transportation Engineering*, 2005, **131**(3): 229-238. DOI:10.1061/(asce)0733-947x(2005)131:3(229).

[8] Im J H, Kim Y R. Performance evaluation of fog seals on chip seals and verification of fog seal field tests [J]. *Canadian Journal of Civil Engineering*, 2015, **42**(11): 872-880. DOI:10.1139/cjce-2014-0340.

[9] Duan D J. Application of synchronous chip seal course in large bridges [J]. *Advanced Materials Research*, 2012, **482-484**: 1073-1077. DOI: 10.4028/www.scientific.net/amr.482-484.1073.

[10] Huang W, Qian Z D, Chen G. Epoxy asphalt concrete paving on the deck of long-span steel bridge [J]. *Chinese Science Bulletin*, 2003, **48**(21): 2391-2394. DOI:10.1360/02ww0123.

[11] Herrington P R, Bagshaw S A. Epoxy modified bitumen chip seals [R]. Wellington: NZ Transport Agency, 2014.

[12] Zhang J P, Luo P F, Xu L, et al. Laboratory study on the permeability and skid resistance of asphalt pavement fog seal layer [C]//*15th COTA International Conference of Transportation Professionals*. Beijing, China, 2015: 949-956.

[13] Ministry of Transport of People's Republic of China. JTG E20—2011 Standard test methods of bitumen and bituminous mixtures for highway engineering [S]. Beijing: China Communications Press, 2011. (in Chinese)

[14] Zhao Z L. Reseacrh on skid resistance technology of asphalt pavement based on fractal method [D]. Xi'an: Chang'an University, 2004. (in Chinese)

[15] Guo Y C, Shen A Q, Zhao X L. Performance evaluation test for fiber asphalt chip seal [C]//*11th International Conference of Chinese Transportation Professionals*. Nanjing, China, 2011: 3434-344.

钢桥面环氧沥青铺装用雾封层加碎石封层的设计与试验评估

郑 冬[1] 钱振东[1] 王 睿[2] 刘 阳[1]

([1] 东南大学智能运输系统研究中心, 南京 210096)

([2] 江苏省苏州市公路管理处, 苏州 215007)

摘要:为了改善钢桥面环氧沥青铺装层(EAP)的表面性能,提出了一种阳离子乳化沥青雾封层与环氧沥青碎石封层(ECS)复合的封层结构,并结合室内试验对复合封层结构进行设计和性能评价. 首先,提出了钢桥面环氧沥青铺装层用碎石封层的评价指标与相应研究方法. 其次,为了最小化封层结构的失效概率,采用小型加速加载设备 MMLS3 和短期老化试验对养护期内最坏路面状况进行模拟. 最后,通过试验分析确定复合封层结构的设计参数,并对所设计的复合封层结构进行性能评价. 结果表明:所提出的路面状况模拟方法是有效的,且作用在 EAP 车辙板上最大的荷载重复次数约为 925 300 次. 此外,复合封层结构可以提供一个密实表面,并且具有足够的抗滑性能、集料沥青间的黏结性能及层间抗剪切性能.

关键词:路面养护;复合封层;环氧沥青;试验评价;路面状况模拟;钢桥面铺装

中图分类号:U418.6